Chengjun Yu, An Deng, Giang D. Nguyen

A constitutive model for cemented geomaterials

Proceedings of the 10th International Conference on Structural Integrity and Failure (SIF-2016): Advances in Materials and Structures, 2016 / Kotousov A, Ma J (ed./s), pp. 202-207

A Constitutive Model for Cemented Geomaterials

Chengjun Yu[1,a*], An Deng[2,b], Giang D. Nguyen[3,c]

[1,2,3] School of Civil, Environmental and Mining Engineering, The University of Adelaide, Australia

[a]chengjun.yu@adelaide.edu.au, [b]an.deng@adelaide.edu.au, [c]g.nguyen@adelaide.edu.au

Keywords: Parallel bond model, constitutive modelling, geo-mechanics, cemented geomaterials.

Abstract. This study presents a constitutive model developed for lightly cemented geomaterials. The cemented geomaterials, when subjected to loading, exhibit hybrid mechanical responses: elastic-brittle due to bond breaking and elastic-plastic due to grains friction. This constitutive model is developed to capture the two mechanical responses by using three physical elements, i.e., the spring, the bond and the slider. These elements are combined to mimic the mechanical responses of lightly cemented soils under triaxial loading conditions. The model formulation is presented and validation with experimental data performed to demonstrate its capability in capturing the material behavior under both low and high confining pressures.

Introduction

Lightly cemented geomaterials are formed by the cementation bonding soil grains. In terms of strength, they fall into a material category between rock (or concrete) and soils. The cementation of soils leads to an increase in uniaxial compressive strength, 100 kPa to 700 kPa, which lies in the gap between rocks and soils. Furthermore, cemented geomaterials undergo a unique mode of failure due to the existence of cementation at particle contacts: the cemented bonds break apart around the contacts when stressed, and then the shear resistance eventually coming into effect through the friction resistance generated at the contacts. A solution to this strength uniqueness was to create an enlarged yield surface for the geomaterials [1, 2]. These test results, however, showed that cemented geomaterials yield completely different from that of soils used to make them, and the volumetric behaviour is always in contraction regardless of the confining pressures acted on the materials. Many other constitutive frameworks were developed by assuming the effects of cementation to be independent of bond state [3-5]. However, this assumption less likely stands due to the fact that the ratio of strength of bonding elements in shear and compression can be different from that of uncemented geomaterials [6]. Albeit improved, recent models established based on the critical state framework still demonstrate some deficiencies in capturing volumetric behaviour of the cemented materials [7-10].

The above unique mechanical characteristic of the cemented geomaterials requires an alternative constitutive framework. The key idea in this paper is to treat the structure of the cemented geomaterials as a combination of two strength components: bonding and friction, which are mimicked by an elastic-brittle body and an elastic-plastic body, respectively. The two mechanical bodies are combined in a form where the progressive failure mode of the cemented geomaterials is captured. The bonding resistance is simulated by Hooke's law, while the friction resistance is simulated by Modified Cam Clay. The latter is further improved by introducing the non-associated flow rule. The progressive failure of the geomaterials is reproduced by defining bond breakage which assesses how the cemented contacts are debonded into frictional masses. The developed constitutive model can capture the increase in stiffness and strength as well as inelastic volumetric behaviour of cemented geomaterials. The model is described in brief in this study.

Characteristics of Cemented Geomaterials

The cemented geomaterials comprise combinations of particle fabrics and contacts bonds. This composition suggests that the material strength stems mainly from the soil skeleton and the cement bonds. The cement bonds are progressively damaged when stressed if the stress exceeds material yielding level [11]. The granulated volume fraction grows leading to friction dominated behaviour with respect to load sharing. This conceptualisation for loading is translated into physical bodies, with the bonds mimicked by the elastic-brittle body and the particles friction being the elastic-plastic body. The friction resistance comes into effect only after a certain amount of material deformation has taken place [12]. The loss of bonding resistance eventually leads to the gain of friction resistance. Based on this understanding, the mechanical response of the lightly cemented geomaterials is further simulated by a combination of ideal mechanical elements, i.e., the spring (elastic deformation), the slider (plastic yielding), and the bonded bar (brittle cracking), as shown in Fig. 1(a). The mechanical elements are characterised in terms of defined modulus or stiffness, i.e., the Young's modulus *E*, the yield strength *f*, and the break strength *q*, respectively. The physical elements are combined into a form shown in Fig. 1(b) which is named a parallel bond unit. The unit consists of an elastic-brittle body which is calibrated by a serial combination of the spring and the bonded bar, and an elastic-plastic body which is a serial combination of the spring and the slider. A breakage ratio, *b*=volume fraction of the elastic-plastic body, is used to characterise the debonding process.

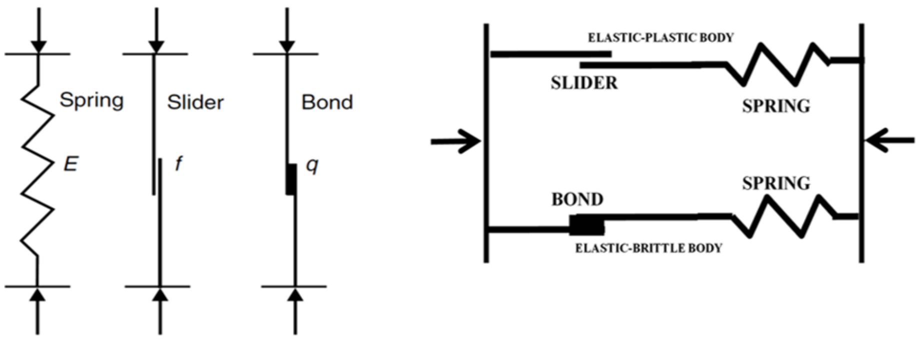

(a) (b)

Fig. 1: Model demonstration: (a) physical elements; (b) parallel unit.

Model Formulation

Further to Fig. 1(b), the stress-strain relationship of the proposed parallel unit is formulated as:

$$p = (1-b)\, p_1 + b p_2 , \tag{1}$$

$$q = (1-b)\, q_1 + b q_2 , \tag{2}$$

where, p and q are the total effective mean stress and the total shear stress, respectively; p_1 and q_1 are the stress components acting on the elastic-brittle body; p_2 and q_2 are the stress components acting on the elastic-plastic body; the corresponding total volumetric strain and total shear strain equal to the strain occurred to the elastic-brittle body and the strain to the elastic-plastic body. Differentiate both sides of Eq. 1 and Eq. 2, and then we have stress increments written as:

$$\partial p = (1-b)\partial p_1 + b\partial p_2 + (p_2 - p_1)\partial b , \tag{3}$$

$$\partial q = (1-b)\partial q_1 + b\partial q_2 + (q_2 - q_1)\partial b . \tag{4}$$

It is shown that the stress increments are composed of three components: the stress increments of elastic-brittle body, the stress increments of elastic-plastic body, and the stress increments due to the cementation breakage. The three stress increment components are described as follows.

Elastic-Brittle Body. The stress increments for the elastic-brittle body are described in terms of Hooke's law:

$$\partial p_1 = K_1 \partial \varepsilon_v , \tag{5}$$

$$\partial q_1 = 3G_1 \partial \varepsilon_s , \tag{6}$$

where K_1 is the bulk modulus and equals the initial tangent slope of mean stress–volumetric strain curve obtained from an isotropic test; G_1 is the shear modulus and equals the initial tangent slope of shear stress–shear strain curve obtained in a triaxial compression test; $\partial\varepsilon_v$ is the corresponding volumetric strain increment; $\partial\varepsilon_s$ is the corresponding shear stain increment.

Elastic-Plastic Body. The stress–strain behaviour of the elastic-plastic body is simulated by introducing the Modified Cam Clay [13]. The yield surface adopted for the elastic-plastic body is assumed to be elliptical and to pass through the origin of the stress coordinate. For triaxial conditions, the yield surface is written as:

$$f = {q_2}^2 + M^2 {p_2}^2 - M^2 p_2 p_0, \tag{7}$$

where M is a constant and equals the aspect ratio of the elliptical yield locus; p_0 is the tip stress. To account for the influence of the cemented structure, a non-associated flow rule is introduced [14], with the plastic potential expressed as:

$$g = {q_2}^2 + \alpha^2 \left({p_2}^2 - {p_p}^2 \right), \tag{8}$$

where α is an experimental parameter defining the shape of the plastic potential; p_p is a parameter defining the magnitude of the plastic potential. The yield surface and plastic potential are illustrated in Fig. 2(a). Fig. 2(b) shows plastic strain incremental vectors. The non-associated flow rule exhibits a degree of flexibility to meet the requirement on volumetric changes. This is achieved by changing the value for α in terms of triaxial test results.

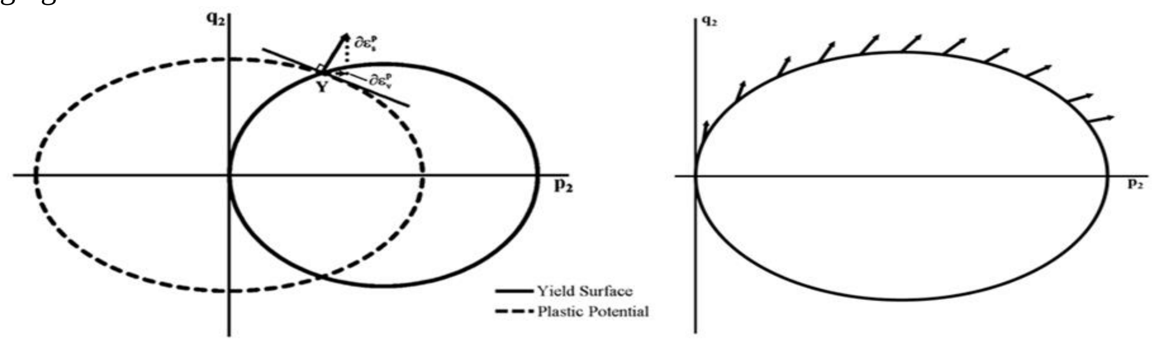

(a) (b)

Fig. 2: Yield surface and non-associative flow rule: (a) yield surface and plastic potential; (b) plastic strain incremental vectors.

The stresses for the elastic-plastic body are integrated by adopting the backward Euler return algorithm, which is known as the semi-implicit scheme [15]. The semi-implicit algorithm is illustrated in Fig. 3. In the case of yielding, a stress state X travels to trial state Y, where the stress increments for the trial are respectively calculated as:

$$\partial {p_2}^{\mathrm{Trial}} = \frac{(1+e)\, {p_2}^X}{\kappa} \partial\varepsilon_v, \tag{9}$$

$$\partial {q_2}^{\mathrm{Trial}} = \frac{9(1-2\nu)}{2(1+\nu)} \left(\frac{(1+e)\, {p_2}^X}{\kappa} \right) \partial\varepsilon_s, \tag{10}$$

where κ is a parameter obtained from unloading tests; ν is material Poison's ratio. At the trial state Y, Eq. 10 is represented through using Taylor expansion as:

$$f = f^{\mathrm{Trial}} + \frac{\partial f}{\partial p_2} \partial p_2 + \frac{\partial f}{\partial q_2} \partial q_2 + \frac{\partial f}{\partial p_0} \partial p_0. \tag{11}$$

The stress incremental forms between states Y and Z are respectively expressed as:

$$\partial {p_2}^{YZ} = -\frac{2\alpha^2 (1+e) \left({p_2}^{\mathrm{Trial}} \right)^2}{\kappa} \partial\lambda, \tag{12}$$

$$\partial {q_2}^{YZ} = -\frac{9(1-2\nu)}{2(1+\nu)} \left(\frac{2(1+e)\, {p_2}^{\mathrm{Trial}} {q_2}^{\mathrm{Trial}}}{\kappa} \right) \partial\lambda, \tag{13}$$

where $\partial\lambda$ is scalar multiplier and obtained by enforcing the yield condition at state *Z* and substituting the proposed flow rule. The stress increments for the elastic-plastic body are then updated as the sum of the trail stress increments from state *X* to *Y* and the stress increment from states *Y* to *Z*:

$$\partial p_2 = \partial p_2^{Trial} + \partial p_2^{YZ} , \tag{14}$$

$$\partial q_2 = \partial q_2^{Trial} + \partial q_2^{YZ} . \tag{15}$$

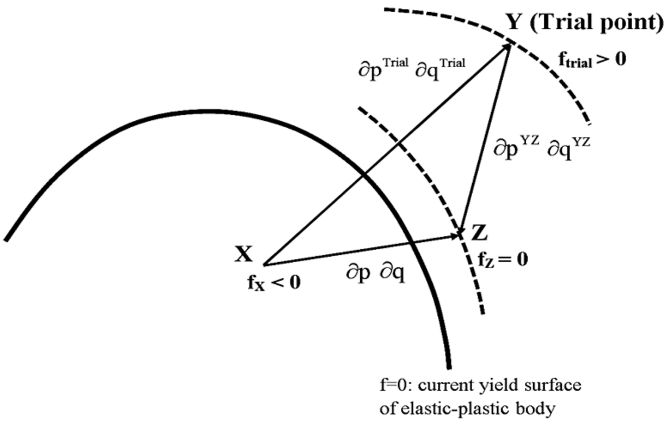

Fig. 3: Stress return algorithm.

Cementation Breakage. The cementation breakage ratio *b* represents the volume fraction for the elastic-plastic body. The value for *b* varies between 0 and 1. To reflect this, the breakage progressing is modelled as a Weibull distribution:

$$b = 1 - e^{-(\beta \varepsilon_d)^2} , \tag{16}$$

where $\varepsilon_d = \sqrt{\varepsilon_v^{p2} + \varepsilon_s^{p2}}$; β is parameter describing variation of the breakage ratio. At the early stage of loading, the geomaterials withstand loads mainly through the elastic-brittle body. The elastic-plastic body comes into effect when the cementation breakage takes place.

Performance of the Simplified Parallel Unit

The proposed parallel unit is validated by comparing model simulation results with test results. The test results were obtained from an investigation conducted on cemented expanded polystyrene (EPS) backfill. Fig. shows the test results, including deviatoric stress–axial strain and volumetric strain–axial strain curves of the cemented EPS backfill. Four series of backfill samples were tested which vary in ingredients dosage and magnitude of confinement pressures. All samples were subjected to consolidated drained triaxial compression tests. Close agreement between the numerical results and the test results in terms of initial stiffness, yield and failure can be seen. In comparison with the Modified Cam Clay model, the proposed model provides better predictions in both low and high confining pressures.

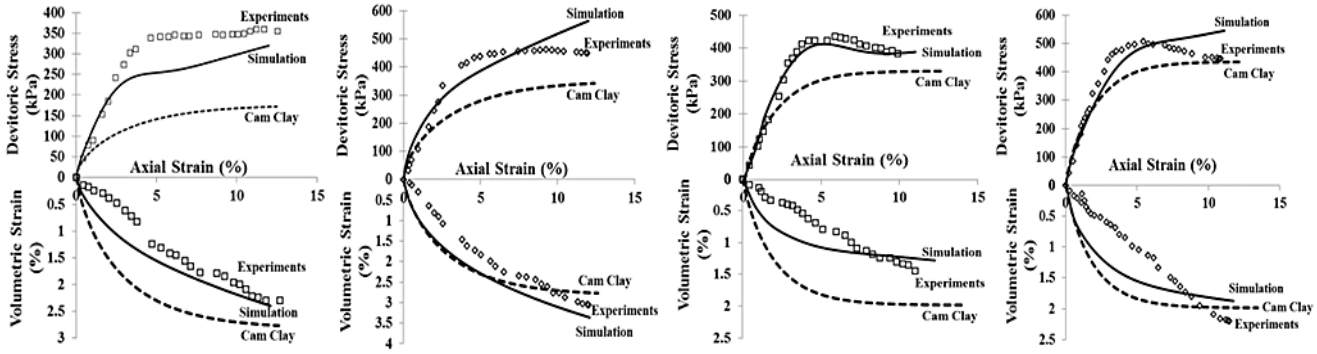

(a) (b) (c) (d)

Fig. 4: Test and model results of stress-strain curves from CD compression for samples (a) cement = 50 kg/m^3, EPS = 4.21 kg/m^3, confinement = 100 kPa; (b) cement = 50 kg/m^3, EPS =2.11 kg/m^3, confinement =200 kPa; (c) cement = 100 kg/m^3, EPS =2.11 kg/m^3, confinement =100 kPa; (d) cement = 100 kg/m^3, EPS =2.11 kg/m^3, confinement =200 kPa.

Conclusions

A constitutive model for lightly cemented geomaterials is presented. The proposed framework takes into account the concurrent interaction between bond breakage and frictional sliding of grains during the material deformation. The two resistance components are mimicked by introducing elastic-brittle body and elastic-plastic body, respectively. Good agreement between numerical and experimental results demonstrates the capability of the proposed approach in capturing the responses of cemented soils under various cement content and confining pressures.

Acknowledgements

This study was supported under Australian Research Council's Discovery Projects funding scheme (project number DP140103004). The views expressed herein are those of the authors and are not necessarily those of the Australian Research Council.

References

1. Leroueil, S. and P.R. Vaughan, *The general and congruent effects of structure in natural soils and weak rocks.* Géotechnique, 1990. **40**(3): p. 467-488.
2. Gens, A. and R. Nova, *Conceptual bases for a constitutive model for bonded soils and weak rocks.* Geotechnical engineering of hard soils-soft rocks, 1993. **1**(1): p. 485-494.
3. Nova, R., R. Castellanza, and C. Tamagnini, *A constitutive model for bonded geomaterials subject to mechanical and/or chemical degradation.* International Journal for Numerical and Analytical Methods in Geomechanics, 2003. **27**(9): p. 705-732.
4. Nova, R., *Modelling of bonded soils with unstable structure*. 2006: Springer.
5. Rahimi, M., D. Chan, and A. Nouri, *Bounding Surface Constitutive Model for Cemented Sand under Monotonic Loading.* International Journal of Geomechanics, 2015: p. 04015049.
6. Vatsala, A., R. Nova, and B.S. Murthy, *Elastoplastic model for cemented soils.* Journal of Geotechnical and Geoenvironmental Engineering, 2001. **127**(8): p. 679-687.
7. Baudet, B. and S. Stallebrass, *A constitutive model for structured clays.* Géotechnique, 2004. **54**(4): p. 269-278.
8. Liu, M.D., J.P. Carter, and D.W. Airey, *Sydney soil model. I: Theoretical formulation.* International Journal of Geomechanics, 2010. **11**(3): p. 211-224.
9. Horpibulsuk, S. and M. Liu, *Structured Cam Clay Model with Cementation Effect.* Geotechnical Engineering Journal of the SEAGS & AGSSEA, 2015. **46**(1): p. 86-94.
10. Kavvadas, M. and A. Amorosi, *A constitutive model for structured soils.* Géotechnique, 2000. **50**(3): p. 263-273.
11. Burland, J., *On the compressibility and shear strength of natural clays.* Géotechnique, 1990. **40**(3): p. 329-378.
12. Shen, Z.-J., *Progress in binary medium modeling of geological materials*. 2006: Springer.
13. Roscoe, K. and K. Burland, *On the generalised stress-strain behaviour of wet clay.* Engineering Plasticity, 1968: p. 535-609.
14. Horpibulsuk, S., et al., *Behaviour of cemented clay simulated via the theoretical framework of the Structured Cam Clay model.* Computers and Geotechnics, 2010. **37**(1): p. 1-9.
15. Simo, J.C., *Numerical analysis and simulation of plasticity.* Handbook of numerical analysis, 1998. **6**: p. 183-499.